UNIVERSIDADE DE SÃO PAULO

INSTITUTO DE FÍSICA
CAIXA POSTAL 20516
01452-990 SÃO PAULO - SP
BRASIL

PUBLICAÇÕES

IFUSP/P-1114

OXYGEN VACANCY CENTERS IN SILICATES. II. DIFFUSION MODEL AND APPLICATION TO BERYL

A. Mizukami, S. Isotani, A.R. Blak, A.W. Mol
Instituto de Física, Universidade de São Paulo

A.R.P.L. Albuquerque
Escola Politécnica, Universidade de São Paulo

Maio/1994

OXYGEN VACANCY CENTERS IN SILICATES. II. DIFFUSION MODEL AND APPLICATION TO BERYL

A. Mizukami, S. Isotani, A.R. Blak, A.W. Mol

Instituto de Física Universidade de São Paulo
C.P. 20.516, 01452-990, São Paulo, SP, Brasil

and

A.R.P.L. Albuquerque

Escola Politécnica, Universidade de São Paulo

Key words: Beryl, Vacancy, Diffusion

Pacs-90: 66.30 Lw

Abstract

The oxygen vacancy F center (an oxygen containing two trapped electrons) thermal decay in beryl, have been investigated by UV OA spectroscopy as a function of isothermal treatments between 600°C and 900°C. A method for the analysis of the thermal decay through a process of diffusion of oxygen vacancy centers and oxygen-vacancy recombination at the free surface have been developed. The resulting differential equation has been solved using standard coordinates separation and expansion methods. The diffusion activation energy from the diffusion of oxygen vacancy centers obtained from the thermal decay analysis is equal to 0.67 eV.

I. INTRODUCTION

In a previous report we showed that the UV bands of spodumene, quartz and beryl are due to electronic transitions of F center (an oxygen vacancy containing two trapped electrons).[1] The F center is one of the most extensively studied intrisinc and radiation induced defects in oxides.[2]

The attribution of some of the bands in the UV region of the OA spectrum to oxygen vacancies is reinforced by the presence of atomic hydrogen in the channels of beryl.[3] UV illumination causes photo-dissociation of OH^- ions, which displaces the hydrogen to an interstitial site. Oxygen vacancies are of fundamental importance in this assumption by allowing the existence of stabilized OH^- ions in the channels adjacent to the vacancies.

Oxygen vacancy is a kind of intrinsic defect that probably has its origin in the crystal growth. Such defect is generally stable at room temperature and is capable of moving to the surface at slightly higher temperatures. The occurence of intrinsic point defects, at any temperature is demanded from thermodynamics.[2] The long life of the crystal and its exposure during these years to a nearly constant oxygen atmosphere pressure, guarantee the thermodynamical equilibrium between concentration of oxygen vacancy centers and oxygen atmosphere.

Oxygen vacancy centers in materials such as quartz, and silica have been extensively studied in association with the development of optical and electronic devices for background radiation environments,[4] such as MOS devices, silica optical fiber guides and quartz oscillators. The porosity of ceramics in nuclear reactors has its origin in the oxygen vacancy mobility through the diffusion of ^{238}P in UO_2 and $(U,Pu)O_2$, making this process strongly dependent on the oxygen pressure.[5,6] Here, in cilindrical samples the combination of vacancy produce macroscopic hollows at the center of the sample.

The objective of this work is the analysis of the thermal decay of oxygen vacancy F center in beryl, by UV OA spectroscopy and diffusion model. The aim is to obtain a better understanding of oxygen vacancy diffusion in oxides.

II. EXPERIMENTAL PROCEDURE

Slices 3mm thick of pink beryl were cut perpendicular to the c-axis. The OA spectra were measured with an unpolarized double beam spectrophotometer ZEISS DMR 21. The isothermal heat treatments were carried out in air, heating and cooling the samples between two metallic plates. Isothermal decay curves were obtained for 550, 700, 800, and 900° C.

Above this temperature, a partial opacity is developed in the samples making it impossible to obtain the OA spectra. Similar opacity was also observed in the work of Goldman et al.[7] Similar heat treatment of quartz and spodumene also shows cracking at 900° C. Topaz with Fe and Cr impurities also show cracking.

In figure 1 the OA spectra of pink beryl is shown: (1) is the spectrum of the untreated beryl, and (2) after heat treatment at 750° C for 55 hours.

INSERT FIGURE 1

Figure 2 shows the normalized thermal decay of the 42000cm^{-1} OA band.

INSERT FIGURE 2

III. THE MODEL OF OXYGEN VACANCY DIFFUSION

The annealing of F centers in the beryl crystal can be done by migration of these centers to the free surface and their subsequent annihilation through atomic oxygen and F center recombination, or by diffusion of oxygen atoms into the crystal network and their subsequent recombination with the F centers.

Atomic diffusion in beryl is most likely to occur through the production of atomic oxygen at the crystal surface followed by their diffusion through the interstitials of the crystal structure. The heat treatment were in air at a constant temperature, and so it is expected a constant rate of production of atomic oxygen. The diffusion through to crystal network implies a long mean diffusion path and as a consequence, a diffusion time longer than that of atom-vacancy recombination time. The analysis using these considerations leads to a dynamical kinetics process problem, which was analysed with a method developed for others kinetics processes.[8-11] The results of the application of this method to the data shown in figure 2 leads to an activation energy of about 0.5 eV, for pure atomic diffusion process.

The beryl crystal grow in a Li rich pegmatite body from magmatic source,[12] similar to that found at Lacorne, Quebec.[13] Then, the beryl crystal grow at conditions of high temperature (above 400°C) and possibly high pressure. In such condition, the atomic diffusion process, lead to small amounts of oxygen vacancies must be found. The long life of the crystal and its exposure during these years to a nearly constant oxygen atmosphere pressure, associated to the small activation energy for the atomic diffusion process, will decrease the remaining F and F^+ centers. So, according with the atomic diffusion model, only neglegible amonts of F and F^+ centers are expected.

Therefore atomic diffusion process is neglected, and only vacancy diffusion process is analysed here.

In equilibrium, F centers will be created or annihilated at the proper surface defects, governed by the equilibrium of the oxygen chemical potentials:

$$2\,\mu_0 = 2\,\mu_{0_2} \quad , \tag{1}$$

where μ_0 is the atomic oxygen chemical potential in the crystal bulk and μ_{0_2} is the molecular oxygen chemical potential in air.

Beryl crystals will be considered to be in an air atmosphere, at a constant temperature,

with a small thickness $2L$ comparative to a large transversal area perpendicular to the c-axis. It will be assumed that there is an initial uniform distribution of F centers and no formation of divacancies at the considered temperature range. The diffusion process will tend to move the F centers to the surface to equalize concentrations. This process will be governed by the first well-known Fick law.[14]

$$\vec{j} = -D\ \mathrm{grad}\ n \tag{2}$$

where $\vec{j}$ is the net current density of defects, $n(x,y,z,)$ the defect concentration density and D the so-called diffusion coefficient which is a function of the thermodynamical conditions.

The vacancy can be produced by displacing a lattice atom; then the released atom can be trapped within the lattice or move out to the surface. For the Frenkel defect, the displaced atom in the interior of the crystal stays at an interstitial site. It will be assumed that Frenkel defects in beryl are only a transient stage and the pair may be created or annihilated with the interstitial moving back to the vacancy site. At the equilibrium condition, the concentration density of F centers, n_b, will be composed primarily of intrinsic F centers but also of oxygen vacancies from Frenkel pairs. If the concentration density, n, of F centers is out of equilibrium, Frenkel pairs are created or annihilated to restore the equilibrium concentration. Then it will be necessary to include a term in equation (1), taking into account the changes introduced by restoring Frenkel pairs. This term vanishes for the equilibrium condition and it will be a function of the difference $n - n_b$. Thus the equation (1) may be rewritten as:

$$\vec{j} = -D\ \mathrm{grad}\, n + \vec{F}\,(n - n_b) \quad , \tag{3}$$

where $\vec{F}$ is the Frenkel pair restoring function.

Taking into account the law of particle conservation, and the crystal form which allows in, first order approximation, consideration of diffusion only along the c-axis, equation (3)

becomes:

$$\frac{\partial n}{\partial t} = D\,\frac{\partial^2 n}{\partial z^2} - \alpha(n - n_b) \quad , \tag{4}$$

where α is the isotropic coefficient of the Frenkel pair restoring function, and n and n_b, respectively, the actual and the equilibrium concentrations.

At the crystal surface the equilibrium current density vanishes. The oxygen in air is in the form of O_2 molecules and in the crystal bulk is in form of O^{2-}, ions not allowing the direct release of O^{2-} ions for the creation of the F centers and the direct absorption of O_2 molecules in the annihilation of F centers. It will be assumed that oxygen is exchanged at the surface in traps of atomic oxygen (O-traps). The equilibrium of $O_2 \rightleftarrows 2O$ from O_2 gas molecules, produces very small amounts of atomic oxygen near the surface, and it is the presence of O-traps that justify a larger concentration of atomic oxygen enough to produce oxygen-vacancy annihilation. Unfortunately, there are no suggestions on O-trap structures, because this is an area which is only briefly discussed, due to the immense difficulty in obtaining high purity and well formed crystals. A suggestion is made in the growth of beryl through the formation of terraces[15], which is consistent with the inherently slow growth of natural crystals along the c-axis forming long hexagonal crystals.

At the crystal surface it is assumed that:

$$j\,|_{\pm L} = \pm h(n - n_b)|_{\pm L} \quad . \tag{5}$$

where h is a coefficient proportional to the rate at which vacancies are exchanged at the surface O-traps. If $n > n_b$, j is positive and a net flux of vacancies is "leaving" the surface with the absorption of oxygen atoms. If $n < n_b$, j is negative meaning that vacancies are being created at the surface from the combination of oxygen ions with trapped oxygen atoms.

From equation (3) and neglecting the Frenkel pair contribution at the surface, equation (5) may be rewritten

$$-D\,\left.\frac{\partial n}{\partial z}\right|_{\pm L} = \pm h\,(n - n_b)|_{\pm L} \quad . \tag{6}$$

Assuming that the initial density $n(t=0) = n_i$ and the condition given by equation (6), the solution of equation (4) (see appendix 1) is:

$$\frac{n(z,t) - n_b}{n_i - n_b} = 2\,e^{-\alpha t} \sum_{j=1}^{\infty} \frac{\sin(\delta_j)\cos(\delta_j z/L)}{\delta_j + \sin(\delta_j)\cos(\delta_j)}\, e^{-\delta^2 j \bar{D} t} \quad , \tag{7}$$

where

$$\cot(\delta_j) = \frac{\bar{D}}{\bar{h}}\,\delta_j \quad , \quad \bar{D} = \frac{D}{L^2} \quad , \quad \bar{h} = \frac{h}{L} \quad .$$

The total concentration of vacancies, n(t), in the sample is then given by the summation over the entire crystal. Integrating along the z-axis from $-L$ to $+L$, the resulting concentration is given by

$$n(t) = n_b + (n_i - n_b)\,e^{-\alpha t}\,F(t) \quad , \tag{8}$$

where n_b and n_i are, respectively, the equilibrium and the initial concentrations, and

$$F(t) = \sum_{j=1}^{\infty} \frac{2\sin^2(\delta_j)}{\delta_j\,[\delta_j + \sin(\delta_j)\cos(\delta_j)]}\, e^{-\delta_j^2 \bar{D} t} \quad .$$

For $n(t=0) = n_i$, $F(0) = 1$.

The OA intensity, $A(t)$, is proportional to the total concentration. Then:

$$\frac{A(t)}{A_0} = \left(1 - \frac{n_b}{n_i}\right) e^{-\alpha t}\,F(t) + \frac{n_b}{n_i} \quad , \tag{9}$$

where $A_0 = A(t=0)$, is a normalization factor.

Considering the summation over 20 terms in equation (9) the fit to the data is shown in figure 2 (solid lines). The values of δ_j are the successive roots of the transcendental equation for δ_j being evaluated using the method of Newton-Raphson.[16]

In table 1, the fitted parameters are shown. Parameters α, $\bar{D}$ and $\bar{h}$ increase with temperature while N_b decreases.

INSERT TABLE 1

IV. TEMPERATURE DEPENDENCE OF DIFFUSION MODEL PARAMETERS

Vacancy diffusion has been already mentioned as an illustrative example of diffusion through successive jumps of atoms into neighboring vacancies. The theoretical calculation of D in terms of the microscopic jump processes is complicated. However, using the random-walk approach a simple general expression for D has been given[17]

$$D = \frac{1}{6}\,\Gamma\, n^2 \quad , \tag{10}$$

where Γ is the jump frequency and n the jump length for cubic lattices.

It may be generally assumed that the jump frequency Γ depends on the temperature according to the law $\Gamma = \Gamma_0\ \exp(-E_m/kT)$, where Γ_0 is an effective frequency and E_m is the height of the energy barrier to be overcome during the jump. Empirically, it is found that D can be described by the equation:

$$D = D_0 \exp(-Em/kT) \quad , \tag{11}$$

where D_0 is a constant. Using $L = 1.5\ 10^{-3}$ m, $D_0 = 8.48 \times 10^{-6}$ cm^2 s^{-1} and $E_m = 0.67$ eV are obtained.

The known E_m values vary from 1 eV for tetravalent transition metal or rare earth MO_2 crystals to $1.7 \sim 3.8$ eV for alkaline-earth MO crystals.[2] The lower energy values

in MO_2 crystals may be a consequence of a smaller metal/oxygen ratio. Assuming this phenomenology to be roughly true, beryl ($Be_3Al_2Si_6O_{18}$) have a metal/oxygen ratio of 11/18 and then a small E_m is expected. It is also known that beryl is a cyclosilicate with large structural channels, facilitating the migration of atoms and lowering the height of the energy barrier. Then the value of 0.67 eV is possibly an acceptable measure of the height of the energy barrier in beryl.

The concentration, n_F, of oxygen vacancies produced by displacing the lattice atoms forming Frenkel are given by

$$n_F \sim (cc')^{1/2} \exp(-E_F/2kT) \quad , \tag{12}$$

where is the number of lattice sites, c' is the number of interstitial sites and E_F is the energy necessary for moving an atom from a lattice site to an interstitial position. The rate of vacancy creation or annihilation, as assumed in equation (3), is proportional to the difference between the equilibrium and the actual concentrations of vacancies. Then, the parameter α will be proportional to c_F and a general expression for α is given by

$$\alpha = \alpha_0 \exp(E_F/2kT) \quad , \tag{13}$$

where α_0 is the frequency factor. Then $\alpha_0 = 0.97$ s^{-1} and $E_F = 2.07$ eV are obtained.

The parameter h from figure 3 is governed by the function

$$h = h_0 \exp(-E_h/2kT) \quad , \tag{14}$$

where $h_0 = 3$ cm/s^{-1} and $E_h = 2.07$ eV. The similarity between E_h and E_F allow the proposition that O-traps behave like interstitial sites during the movement of an oxygen atom when a Frenkel pair is created.

V. TEMPERATURE DEPENDENCE OF VACANCY EQUILIBRIUM

A thermodynamic calculation of the equilibrium concentration of oxygen vacancies in a crystal at a given T and P, will be such that the Gibbs free energy function G will be a minimum. Then, the chemical potential vanishes and a simple relation is obtained relating the G function for the formation of a vacancy, N atoms and n_b.[17] However for the calculation of n_b, the chemical potential of the O_2 gas molecules near the crystal surface is necessary. In this case, the use of a statistical mechanical approach will give a better description of the chemical potential.

The temperature dependence of the equilibrium concentration N_b using a statistical mechanics approach [18] is now considered. The chemical potential of the molecular oxygen gas, at high temperatures includes translation, rotation, vibration, the electronic state without excitation, degeneracy of the fundamental state and degeneracy of the nuclear spin ($I = 0$). It will be assumed that the partition function is particle independent. Using the well known partition function for each contribution and the Stirling approximation, the chemical potential of the molecular oxygen gas is given by

$$\mu_{O_2} = -kT \ln \left\{ \frac{(2\pi\, kT)^{7/2}\, I m_{O_2}^{3/2}}{2h^5\, P_{O_2}} \frac{e^{-\epsilon_{O_2}/kT}}{\sinh\left(\frac{\omega_{O_2}\hbar}{2kT}\right)} \right\} \quad , \tag{15}$$

where I is the moment of inertia, ϵ_{O_2} is the electronic energy of the ground state and ω_{O_2} is the angular frenquency of the stretching vibration of the oxygen molecule. P_{O_2} is the partial pressure of the oxygen gas and m_{O_2} is the mass of the oxygen molecule.

The chemical potential of the atomic oxygen in the crystal lattice, assuming "independent particle approximation" and including the ground electronic state and vibrations, is given by

$$\mu_{O_2} = -kT \ln \left\{ \frac{N_0 - N}{N} \frac{e^{-\epsilon_0/kT}}{\prod_{i=1}^{3} 2\sinh\left(\frac{\omega_i\hbar}{2kT}\right)} \right\} \quad , \tag{16}$$

where N_0 is the number of vacant sites in the lattice for oxygen occupation, N is the number of oxygen occupied sites, ϵ_0 is the site electronic bonding energy and ω_i is the vibrational angular frequency along the three directions.

From equations (1), (15) and (16) one obtains

$$\frac{N}{N_0 - N} = f(T) \quad , \tag{17}$$

where

$$f(T) = \frac{2^{1/2}\, \hbar^{5/2}\, P_{O_2}^{1/2}}{(2\pi\, kT)^{7/4}\, J1/2\, m_{O_2}^{3/4}} \frac{\sinh^{1/2}\left(\frac{\omega_{O_2}\hbar}{2kT}\right)}{\prod_{i=1}^{3} 2\sinh\left(\frac{\omega_i\hbar}{2kT}\right)} e^{\left(\epsilon_{O_2}/2 - \epsilon_0\right)/kT} \quad .$$

As $N/(N_0 - N) = (N_0 - N_b)/N_b$ the expression for the temperature description for n_b becomes

$$\frac{N_b}{N_i} = \frac{N_0/N_i}{1 + f(T)} \quad . \tag{18}$$

Assuming $J = 19.1 \times 15^{-47}$ kg m^2, $P_{O_2} = 1$ atm, $m_{O_2} = 5.32 \times 10^{-26}$ kg and $\omega_{O_2} = 2.98 \times 10^{14}\, s^{-1}$ and considering the oxygen vibration similar to the molecular oxygen vibration $\omega_{O_2} = \omega_3$ and the other two $\frac{\omega_{1,2}\hbar}{k} < 100$, an expression for $f(T)m$ is obtained

$$f(T) = \frac{0.168}{T^{7/4}} \frac{e^{\left(\epsilon_{O_2}/2 - \epsilon_0\right)kT}}{\left(\frac{\omega_1}{2kT}\right)\left(\frac{\omega_2\hbar}{2kT}\right)\sinh^{1/2}\left(\frac{1138}{T}\right)} \quad , T > 100 \quad \text{(Kelvin)} \quad . \tag{19}$$

In figure (4) the fit of the values of N_b/N_i with $(\epsilon_{O_2}/2 - \epsilon_0)/k = -3.017\ 10^3$ (Kelvin) is shown, for $\omega_1\omega_2\hbar^2/(4k^2) = 0.053$ (Kelvin^2) and $N_0/N_i = 1.00005$.

INSERT TABLE 4

Assuming that the electronic energy of the ground state of the oxygen molecule is the bond energy plus the zero point oscillation energy, the oxygen ion bonding energy in the crystal is $\epsilon_0 = -2.34$ eV.

The fit the values of N_b/N_i and those calculated from equation (19) is quite reasonable. However, the variation of N_b/N_i with temperature suggests an abrupt decay vanishing at about 1200 K, while equation (19) show a slow decay for higher temperatures.

The opacity observed at temperatures above 1200 K could be explained by the formation of bubbles, through the aggregation of vacancies, followed by localized stress and cracking of the crystal. This interaction between vacancies introduces a new mechanism for the decay of vacancies. Assuming that this interaction will also increase the exchange mechanism of oxygen at surface, the value of the equilibrium concentration will be lowered.

VI. CONCLUSIONS

The decay-kinetics analysys of the UV bands of beryl led to conclusions which can be summarized as below:

(a) The oxygen vacancy diffusion model agrees better with the known beryl crystal grow process.

(b) The oxygen vacancy are formed by the displacing oxygen ions into the interstitials (Frenkel pairs) and oxygen loss at the crystal surface.

(c) The activation energy for the F center diffusion in beryl is consistent with the empirical metal oxygen ratio observed in alkaline-earth oxydes.

(d) The activation energy for oxygen displacing is similar to that value found for surface loss, suggesting that both process are similar.

(e) The equilibrium concentration calculation show a good adherence with those obtained from thermal decay analysis.

ACKNOWLEDGMENTS.

This work was partially supported by Conselho Nacional de Desenvolvimento Científico e Tecnológico (CNPq), Fundação de Amparo à Pesquisa do Estado de São Paulo (FAPESP) and Financiadora de Estudos e Projetos (FINEP).

APPENDIX 1 — Solution of the Diffusion Equation

Solution of diffusion equations are not so connon for this films. Therefore a detailed solution of the diffusion equation (4) is shown here.

Taking the transformation $n - n_b = \Omega\, e^{-\alpha t}$, equation (4) becomes:

$$\frac{\partial \Omega}{\partial t} = D\,\frac{\partial^2 \Omega}{\partial z^2} \quad , \tag{A.1}$$

with $\Omega_i = n_i - n_b$ at $t = 0$ and

$$-\,D\,\frac{\partial \Omega}{\partial z}\,|_{\pm L} = \pm h \Omega|_{\pm L} \quad . \tag{A.2}$$

By separation of variables

$$\Omega(z,t) = u(z)\,v(t) \quad , \tag{A.3}$$

from equation (A.1), the following equations are obtained

$$\frac{d}{dt}\,v(t) \;=\; -\lambda^2\,D\,v(t) \quad , \tag{A.4}$$

$$\frac{d^2}{dz^2}\,u(z) \;=\; -\lambda^2\,u(z) \quad , \tag{A.5}$$

where λ^2 is a constant.

The solution of (A.4) is proportional to $\exp(-\lambda^2 D t)$. The solution of (A.5) is a linear combination of $\cos(\lambda z)$ and (λz). Then the general solution of (A.1) is given by:

$$\Omega_\lambda(z,t) = e^{-\lambda^2 D t}\,A_\lambda \cos(\lambda z) + B_\lambda \sin(\lambda z) \quad . \tag{A.6}$$

For longer periods of time, it is assumed that $n \rightarrow n_b$, i.e., the concentration of vacancies reaches an equilibrium concentration for which n_b and Ω must vanish. Satisfying this condition, λ must be real.

From (A.2) and (A.6) for $z = -L$

$$-\,A_\lambda \lambda \sin(\lambda L) - B_\lambda \lambda \cos(\lambda L) = -\frac{h}{D}\,\{A_\lambda \cos(\lambda L) - B_\lambda \sin(\lambda L)\} \quad , \tag{A.7}$$

and for $z = L$

$$A_\lambda \lambda \sin(\lambda L) - B_\lambda \lambda \cos(\lambda L) = \frac{h}{D}\,\{A_\lambda \cos(\lambda L) + B_\lambda \sin(\lambda L)\} \quad . \tag{A.8}$$

From the sum and the difference of (A.7) and (A.8):

$$B_\lambda \lambda \cos(\lambda L) \;=\; -B_\lambda\,\frac{h}{D}\sin(\lambda L) \quad , \tag{A.9}$$

$$A_\lambda \lambda \sin(\lambda L) \;=\; A_\lambda\,\frac{h}{D}\cos(\lambda L) \quad . \tag{A.10}$$

Two cases are possible. The first is assuming $B_{\lambda \neq 0}$, from (A.9) and (A.10):

$$\mathrm{tg}(\lambda L) = -\frac{D}{h}\,\lambda \tag{A.11}$$

$$A_\lambda \sin(\lambda L)\left\{\lambda^2 + (\frac{h}{D})^2\right\} = 0 \quad . \tag{A.12}$$

If $\lambda \neq 0$, from (A.12) $A_\lambda = 0$. Equation (A.11) has a solution for $\lambda = 0$, and from (A.10) $A_{\lambda=0} = 0$. As the negative solutions of λ do not introduce new solutions,

$$\Omega_1(z,t) = \sum_{\lambda_{1,n}>0} e^{-\lambda_{1,n}^2 D t}\,B_{\lambda_{1,n}}\,\sin(\lambda_{1,n} z)$$

where

$$\mathrm{tg}(\lambda_{1,n} L) = -\frac{D}{h}\,\lambda_{1,n} \quad .$$

In the second case, $A_\lambda \neq 0$, and now using similar arguments as discussed above, $B_\lambda = 0$. The solution is then

$$\Omega_2(z,t) = \sum_{\lambda_{2,n}>0} e^{-\lambda_{2,n}^2 D t}\,A_{\lambda_{2,n}}\,\cos(\lambda_{2,n} z)$$

where

$$\mathrm{cotg}(\lambda_{2,n} L) = \frac{D}{h}\lambda_{2,n} \quad .$$

The general solution is $\Omega = \Omega_1 + \Omega_2$. The coefficients $A_{\lambda_{2,n}}$ and $B_{\lambda_{1,n}}$ are determined from the initial conditions $\Omega(z,0) = \Omega_i$ =constant, taking into account that $\sin(\lambda_{1,n} z)$ and

$\cos(\lambda_{2,n}z)$ are orthogonal functions,

$$B_{\lambda_{1,n}} = 0$$

$$A_{\lambda_{2,n}} = \frac{2\Omega_i \sin\delta_n}{\delta_n + \sin\delta_n \cos\delta_n}$$

where $\delta_n = \lambda_{2,n}L$. The general solutions is:

$$\Omega(z,t) = 2\Omega_i \sum_n e^{-\delta_n^2 \frac{D}{L^2}t} \left\{ \frac{\sin\delta_n}{\delta_n + \sin\delta_n \cos\delta_n} \right\} \cos\left(\frac{\delta_n z}{L}\right) = (n - n_b)\, e^{\partial t}$$

with

$$\operatorname{cotg}\delta_n = \frac{D}{hL}\delta_n \quad .$$

REFERENCES

[1] S. Isotani, W. Bonventi Jr., K. Watari, A. Mizukami, A.R. Black, A.S. Ito and A.R.P.L. Albuquerque, *Phys. Rev.*, submitted.

[2] F. Agullo-Lopez, C.R.A. Catlow, P.D. Townsend, "Point Defects In Materials", Academic Press, London, San Diego (1988) p.3, 156.

[3] A.R. Blak and S.W.S. McKeever, *Rad. Prot. Dosimetry* in press.

[4] S.W.S. McKeever, *Rad. Protect. Dos.* **8**, 81 (1984).

[5] D.G. Leme "Cationic Interdiffusion in UO_2 - $(U,Pu)O_2$ and UO_2 - PuO_2 Systems", Ph. D. Thesis, Institute of Physics at the University of São Paulo (1985).

[6] Hj. Matzke, "Diffusion in Non-stoichimetric Oxides". In: T. Sorensen, "Non-stoichimetric Oxides". Academic Press, New York (1981), 155.

[7] D.S. Goldman, G.R. Rossman and K.M. Parkin, *Phys. Chem. Minerals* **3**, 225 (1978).

[8] J.H.S. Sá, "Litiniferous Pegmatites from Itinga-Araçuaí, Minas Gerais", Ph. Thesis at São Paulo University (1977).

[9] H.A. Siroonian, D.M. Shaw and R.E. Jones, *Canad. Mineral.*, **6**, 320 (1959).

[10] R. Antonini, S. Isotani, W.W. Furtado, W.M. Pontuschka and S.R. Rabbani, *An Acad. Bras. Ci.*, **62**, 39 (1990).

[11] S. Isotani, A.T. Fujii, R. Antonini, W.M. Ponstuschka, S.R. Rabbani and W.W. Furtado, *An Acad. Bras. Ci.*, **62**, 107 (1990).

[12] S. Isotani, W.W. Furtado, R. Antonini and O.L. Dias, *Am. Mineral* **74**, 432 (1989)

[13] S. Isotani, W.W. Furtado, R. Antonini, A.R. Blak, W.M. Pontuschka, T. Tomé and S.R. Rabbani, *Phys. Rev.* **B42**, 5966 (1990).

[14] A. Fick, *Ann. Phys. Chem.* **4**, 59 (1855).

[15] E. Schonherr, "The Growth of Large Crystals from the Vapor Phase". In: "Growth, Properties and Applications". Springer-Verlag, Berlin, Heidelberg, New York (1980).

[16] W.H. Press, B.P. Flannery, S.A. Teukolsky, W.T. Vetterling, "Numerical Recipes in C.The Art of Scientific Computations," Cambridge University Press, Cambridge (1988).

[17] R.E. Howard and A.B. Lidiard, *Rep. Prog. Phys.* **27**, 161 (1964).

[18] H.B. Callen, "Thermodynamics and an Introduction to Thermostatistics", John Wiley & Sons, New York (1985).

FIGURE CAPTIONS

Figure 1. OA spectra in the UV region for untreated pink beryl and thermally treated at 750° for 55 hours.

Figure 2. Decay curves of the UV optical absorption band at 42000 cm^{-1} for isothermal treatments at 550, 700, 800 and 900°.

Figure 3. Temperature dependence of the relative vacancy equilibrium concentration N_b/N_i as compared with the thermodynamical calculation.

Table 1 — The Fitted Parameters $\alpha, \bar{D}, \bar{h}$ and N_b/N_i.

T (K)	α (10^{-5} s^{-1})	$\bar{D}$ (10^{-5} s^{-1})	$\bar{h}$ (10^{-5} s^{-1})	N_b/N_i
823	0.043	0.30	9.47	0.730
973	0.417	1.30	85.63	0.630
1073	1.295	2.77	276.5	0.545
1173	3.462	4.88	724.1	0.385

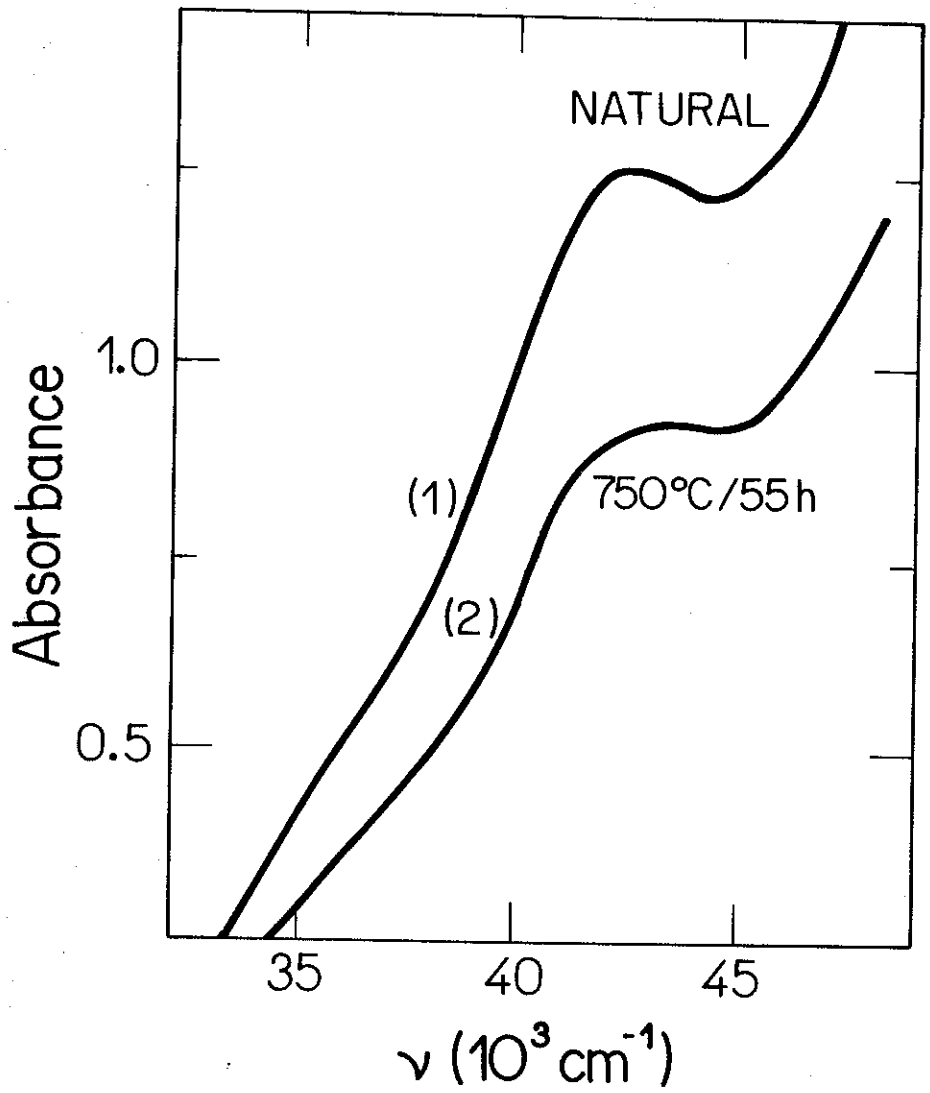

Oxygen vacancy II
A. Mizukami et al
Phys. Rev.

Fig 1

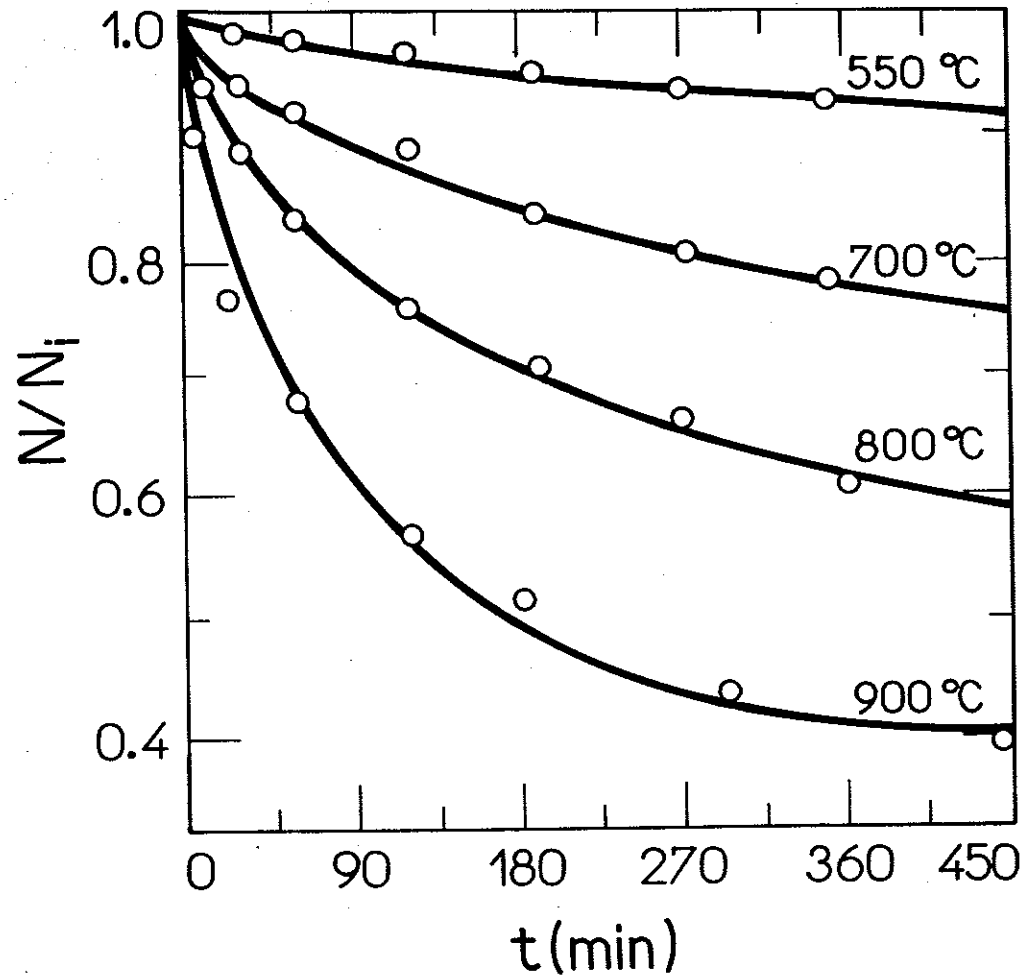

Oxygen vacancy II
A. Mizukami et al.
Phys. Rev.

Fig 2

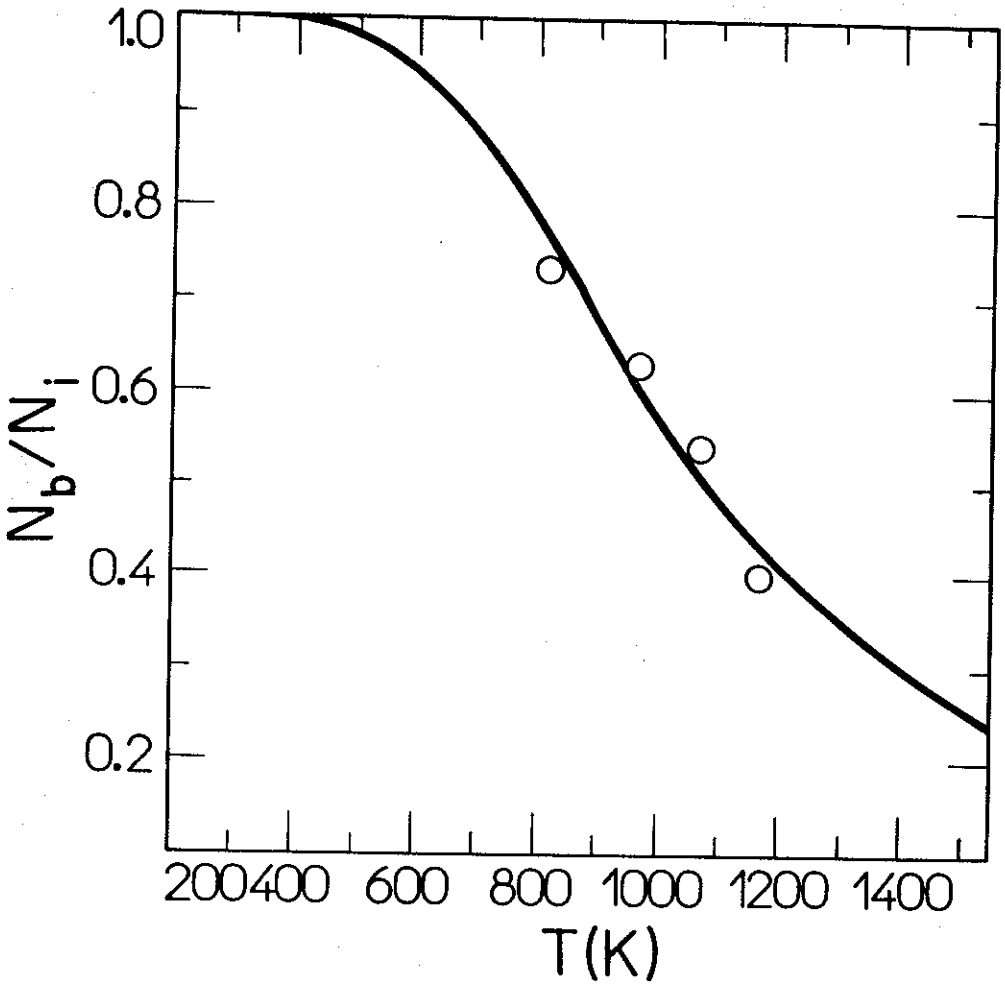

Oxygen vacancy II.
A. Mizokami et. al.
Phys. Rev.

Fig 3